

111 51
52275
P-29

NASA TECHNICAL MEMORANDUM 104163

**MEASUREMENTS OF FUSELAGE SKIN STRAINS
AND DISPLACEMENTS NEAR A LONGITUDINAL
LAP JOINT IN A PRESSURIZED AIRCRAFT**

Edward P. Phillips and Vicki O. Britt

OCTOBER 1991



National Aeronautics and
Space Administration

Langley Research Center
Hampton, Virginia 23665

(NASA-TM-104163) MEASUREMENTS OF FUSELAGE
SKIN STRAINS AND DISPLACEMENTS NEAR A
LONGITUDINAL LAP JOINT IN A PRESSURIZED
AIRCRAFT (NASA) 29 p CSCL 20K

N92-13455

Unclas
G3/39 0052275

MEASUREMENTS OF FUSELAGE SKIN STRAINS AND DISPLACEMENTS NEAR A LONGITUDINAL LAP JOINT IN A PRESSURIZED AIRCRAFT

ABSTRACT

Strains and displacements in a small area near a longitudinal lap joint in the fuselage skin of a B737 aircraft were measured during a pressurization cycle to a differential pressure of 6.2 psi while the aircraft was on the ground. Strain gages were placed on both the inside and outside surfaces of the fuselage at the same locations. Direct Current Differential Transformers (DCDTs) were distributed circumferentially across the lap joint on the inside of the aircraft to measure the relative radial displacements of the skin. The major trends in the results were: (1) hoop strains were higher than longitudinal strains at each location, (2) membrane strains in the unreinforced skin were higher than in the joint, (3) membrane strains in the hoop direction, as well as radial displacements, tended to be highest at the mid-bay location between skin reinforcements, (4) significant bending in the hoop direction occurred in the joint and in the skin near the joint, and the bending was unsymmetrically distributed about the stringer at the middle of the joint, and (5) the radial displacements were unsymmetrically distributed across the lap joint. The interpretation of the strain gage data for locations on the bonded and riveted lap joint assumed that the joint did not contain disbanded areas.

INTRODUCTION

An analytical and experimental program is underway at the NASA Langley Research Center to study multi-site fatigue cracking in fuselage skin joints. A major goal of the study is to develop and verify the methodology necessary to predict the fatigue crack growth behavior of the joints. The methodology required can be divided into two parts: (1) structural analyses capable of quantifying the stresses, including local bending deformations, in the joints, and (2) a crack growth model capable of predicting the growth of cracks given accurate stress analysis results. The current plan is to verify the second part (crack growth model) using the results of fatigue tests of simple flat panels that incorporate a skin joint and that are loaded in the plane of the skin by mechanical testing machines. Though loaded in-plane, some local bending normally occurs in the joints and the effect of that bending on the crack growth behavior of the joints is of particular interest in the Langley study. By documenting the bending in the test specimens, it should be possible to verify the capability of the crack growth model to account for the bending. However, it is recognized that the bending that occurs in the flat test panels will not be the same as the bending that occurs in an actual fuselage structure loaded by internal pressure. To obtain some idea of the differences that could be expected between the test panels and actual structure, and to

obtain data that could be used to help verify structural analysis methods, strain and displacement measurements on an actual aircraft fuselage during a pressurization cycle were needed.

An early model Boeing 737 aircraft used for flight research at Langley was made available for the strain and displacement measurements for a brief period between scheduled flight programs. The short period of access to the aircraft limited the scope of the measurements to 36 total channels of strain gage data divided between inside and outside skin surfaces, and eleven Direct Current Differential Transformer (DCDT) measurements on the inside skin surface. The strain gages were all located in about a 5 inch by 5 inch area near a longitudinal lap joint in the fuselage skin and the DCDTs were aligned along a 19-inch arc across the lap joint. Measurements were taken during a pressurization to a differential pressure of 6.2 psi while the aircraft was on the ground. The results of the strain and displacement measurements are documented in this report.

TEST PROCEDURES

The area chosen to be instrumented with strain and temperature sensors was near a longitudinal lap joint on the upper, aft portion of the right side of the fuselage as indicated in Figure 1. The instrumented area was between Body Stations 847 and 867 (Body Station is the distance in inches along the length of the fuselage from a forward reference point) at 80 to 90 inches above the cabin floor. This location was chosen to be instrumented because it is close to existing, sealable ports in the fuselage through which the sensor cables could be routed. The longitudinal lap joint in this aircraft was fabricated by overlapping adjacent 0.036 inch thick skin segments (2024-T3 Alclad aluminum alloy) of the fuselage and then both adhesively bonding and riveting the skin together. The precise locations of the strain and temperature sensors relative to the lap joint and structural members on the inside of the fuselage are shown in the sketch in Figure 2. Sensor installations shown on the inside of the fuselage were duplicated on the outside of the fuselage at the same locations. The only exception to this was the two strain gages located at Body Station 865 (BS865). Due to an installation error, the gages on the inside and outside were displaced from each other by 0.10 inch in the longitudinal direction. Photographs of the sensor installations are shown in Figure 3. As shown in the photographs, the primer and paint were removed from the surfaces before installation of sensors.

The bonded foil strain gages were 350 ohm, 0.125 inch gage length, and self-temperature-compensated for application on aluminum alloys. Two-element and three-element rosettes were made by stacking individual gages. All strain gages were connected to a digital data acquisition system located external to the aircraft through conventional 3-wire cables that were approximately 65 feet long. The temperature sensors were the bonded foil type. Power had been applied to the sensors long

enough for the outputs to stabilize before the test cycle was begun. All strain gage bridges were zeroed just before start of the pressure cycle.

The area selected for radial deflection measurements was located near Body Station 847 adjacent to the area instrumented with strain and temperature sensors. Positioned below the selected area was a free standing test apparatus consisting of a tripod base and an aluminum extension arm which supported a curved aluminum panel that supported the eleven DCDTs. The apparatus was situated so that the panel supporting the DCDTs was located 3 inches below the fuselage skin and extended across the lap joint as shown in Figure 4. A photograph of the DCDTs in position on the aircraft is shown in Figure 5. The DCDTs were connected to a data acquisition system located external to the aircraft using wires that were approximately 80 feet long.

The fuselage was pressurized on the ground using the aircraft auxiliary power unit. The outputs of digital absolute pressure sensors located inside and outside the fuselage were recorded with every scan of the strain and temperature sensors. The time history of the differential pressure is shown in Figure 6, where the peak differential pressure of 6.2 psi was reached about 17 minutes after start of pressurization.

Two ultrasonic inspections (different inspectors) were performed on the strain gaged portion of the lap joint after the measurement pressure cycle. Both inspections indicated some areas of disbond in the joint, but the two inspections did not always identify the same locations as being disbanded. The actual status of the bond in the joint remains in question. Obviously, if disbonds actually exist at or near strain gage locations, the measured strains may not accurately represent the behavior of a fully bonded joint.

RESULTS

The results of the strain and displacement measurements are presented in this section in graphical form to illustrate trends due to differential pressure (ΔP) and to location. Results are presented for both membrane and bending strains and for both hoop and longitudinal directions, but with emphasis on bending in the hoop direction. For locations where both hoop and longitudinal strains were measured, stresses at maximum ΔP were computed and are plotted to show trends with location. For locations within the lap joint, the membrane and bending strains that are plotted should be interpreted as "apparent" membrane and bending strains because the assumption has been made that the two sheets that overlap to form the joint are completely bonded and respond structurally as a monolithic sheet.

Measured Strains

Error Due to Temperature Change. - The temperature sensors bonded to the inside and outside surfaces indicated that the skin temperature changed by only 8 to 9 degrees Fahrenheit during the pressure cycle. The inside and outside skin temperatures were always within 1 degree Fahrenheit of each other. Since the gage alloy used gives self temperature compensation for aluminum alloys, the temperature change measured during the test would cause less than a 10 microinch/inch error in indicated strain between the start and finish of the pressure cycle. Considering the small maximum error, the strain data were not corrected for error induced by temperature.

Membrane Strains. - Hoop and longitudinal membrane strains measured at several locations at BS862 are plotted against ΔP in Figure 7. All of the hoop strain curves are reasonably linear with ΔP , but the longitudinal strain curves exhibit a small degree of nonlinearity. The strains at maximum ΔP are plotted against distance above the bottom edge of the lap joint in Figure 8. In Figure 8, BRR and TRR refer to the bottom row of rivets and top row of rivets locations respectively. As expected, the hoop strains in the skin away from the joint are substantially larger than those in the joint area, and the hoop strains are larger than the longitudinal strains. The hoop membrane strains at maximum ΔP are plotted against distance forward of BS867 (location of ring stiffener) in Figure 9. The general trend in Figure 9 is for the strains in the unreinforced skin to be slightly higher at the mid-bay location (BS862) between skin reinforcements than in the other areas examined.

Bending Strains. - In this report, the convention used to indicate direction of bending at a gaged location was to define the bending strain to be equal to (outside strain - inside strain)/2. Hoop and longitudinal bending strains measured at several locations at BS862 are plotted against ΔP in Figure 10. All of the bending strain curves are nonlinear with ΔP and exhibit quite different characteristics from location to location. Even the strain curves measured at several body stations at the same distance (0.16 inch) above the top edge of the lap joint exhibit different characteristics (see Figure 11).

Ratio of Bending to Membrane Strains. - To identify the locations where the bending strains are significant compared to the membrane strains, the bending data have been plotted in terms of the ratio of bending to membrane strains. The sign of the ratio reflects the sign of the bending strains since all of the membrane strains are positive (tensile). The bending/membrane strain ratios for the hoop and longitudinal directions are plotted against distance above the bottom edge of the joint in Figure 12, and the hoop direction ratio is plotted against distance forward of BS867 in Figure 13. The data in Figure 12 indicate significant bending in the hoop direction at both the top and bottom rows of rivets (TRR and BRR) in the joint and in

the skin close to the edge of the joint. The bending was found to be unsymmetrically distributed about the stringer at the middle of the joint, as should be expected considering that the signs of the bending strains due to the eccentricity of the skin lap and the bending strains due to pressure pillowing are the same on the bottom side of the joint but not on the top side. The ratio of bending to membrane strains exceeded -1.0 at the bottom row of rivets, indicating that the outside surface was in compression at maximum ΔP . The data in Figure 13 suggest a weak trend towards more significant bending near the ring stiffener at BS867 than at locations away from BS867, but much of the change in the bending/membrane strain ratio is due to changes in the membrane strain.

Stresses

Stresses were computed for the four locations that had gages in both the hoop and longitudinal directions. Stresses were assumed to be zero in the skin thickness direction, so the stresses were computed from the measured strains from:

$$\sigma_H = E(\epsilon_H + \mu \epsilon_L) / (1 - \mu^2) \text{ and } \sigma_L = E(\epsilon_L + \mu \epsilon_H) / (1 - \mu^2)$$

where,

σ_H and σ_L are hoop and longitudinal stresses, respectively

ϵ_H and ϵ_L are hoop and longitudinal strains, respectively

E is Young's modulus (assumed to be 10.6×10^6 psi)

μ is Poisson's ratio (assumed to be 0.33)

The computed membrane stresses for the hoop and longitudinal directions at $\Delta P = 6.2$ psi are plotted against distance above the bottom edge of the joint in Figure 14. Similarly, the ratios of bending to membrane stress are plotted in Figure 15. For the hoop direction, the trends in the stresses were similar to the trends in the strains, but the trends in the stresses and strains were somewhat different for the longitudinal direction. The ratio of the hoop to the longitudinal membrane stresses at $\Delta P = 6.2$ psi for the four locations is plotted in Figure 16. The values range from 1.3 at the top row of rivets to 1.85 at one of the skin locations.

Principal stresses were calculated for the 45 deg. rosette locations and were found to be essentially the same as the stresses in the hoop and longitudinal directions. The maximum stress calculated for any location was 13.8 ksi at the inside surface of the skin at BS865.9, 0.16 inch above the top of the joint.

Displacements

The measured radial deflection of the fuselage skin spanning the lap joint is shown in Figure 17. The deflection is plotted at differential pressures varying from 1 psi to 6 psi. The

deflection in the center of the bays between stringers is much higher than in the areas where the skin is reinforced by the attached stringers. The deflection pattern is not symmetric about the center of the lap joint due to the eccentricity introduced by the joint itself. The measured deflections are higher between stringers 3R and 4R than between stringers 4R and 5R. In order to explain these measured deflection patterns, a detailed structural analysis model including global aspects of the aircraft such as floor rotation and variations in frame height would be needed and a geometrically nonlinear shell analysis should be conducted.

DISCUSSION

The results from the limited strain and displacement measurements performed during this test are in general agreement with expected trends. While the general trends were as expected, the trends could not be accurately quantified because of the limited number of strain and displacement measurement locations and some apparent inconsistencies observed in the strain data. Particular inconsistencies of note are evident in the results shown in Figures 8 and 9. In Figure 8, the hoop membrane strains measured at the bottom row of rivets and top row of rivets at BS862 are significantly different (ratio of 1.25). This result does not seem reasonable for a well bonded joint. Also in Figure 8, the hoop membrane strain shown at 0.16 inch above the top edge of the joint at BS862 is substantially lower than the strains at the other two skin locations at that body station. The low value measured at BS862, 0.16 inch is also evident in Figure 9 where it does not fit the trend of the other measurements at 0.16 inch above the joint edge. Although the causes of the apparent inconsistencies in the strain data discussed above are not known, both could have been caused by nonuniform load transfer due to disbonds in the joint. The radial displacement pattern shown in Figure 17 indicates that the displacements in the skin were higher on the upper side of the lap joint than on the lower side. It is evident that bending occurs in the lap joint, but due to the fact that only three DCDTs were located on the joint itself, the nature of the deflection pattern could not be exactly described by the experimental data.

CONCLUDING REMARKS

Strains and displacements in a small area near a longitudinal lap joint in the fuselage skin of a B737 aircraft were measured during a pressurization cycle to a differential pressure of 6.2 psi while the aircraft was on the ground. Strain gages were placed on both the inside and outside surfaces of the fuselage at the same locations. Direct Current Differential Transformers were placed in a row across the lap joint to measure the radial deflections of the skin. The major trends in the results were: (1) hoop strains were higher than longitudinal strains at each location, (2) membrane strains in the unreinforced skin were higher than in the joint, (3) membrane strains in the hoop direction, as well as radial displacements, tended to be higher

at the mid-bay location between skin reinforcements, (4) significant bending in the hoop direction occurred in the joint and in the skin near the joint, and the bending was unsymmetrically distributed about the stringer at the middle of the joint, and (5) the radial displacements were unsymmetrically distributed across the lap joint. The current interpretation of the data for gage locations on the lap joint may be misleading if the joint was not fully bonded. The actual status of the bond in the joint in the strain gaged area remains in question. Strain data from several other locations on the joint are needed to firmly establish the strain behavior of the joint.

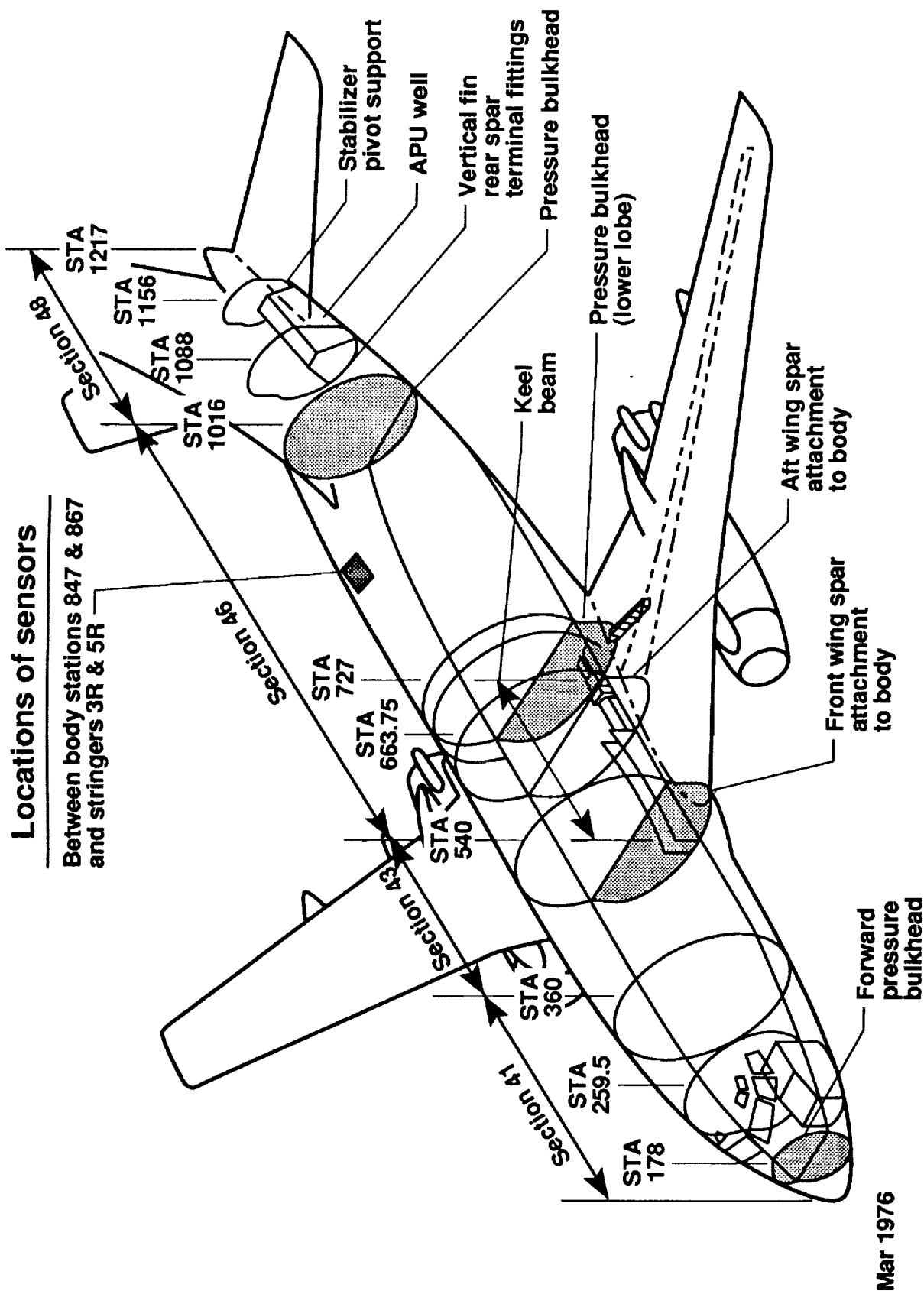


Figure 1. General locations of strain, displacement, and temperature sensors on the fuselage of B737 aircraft.

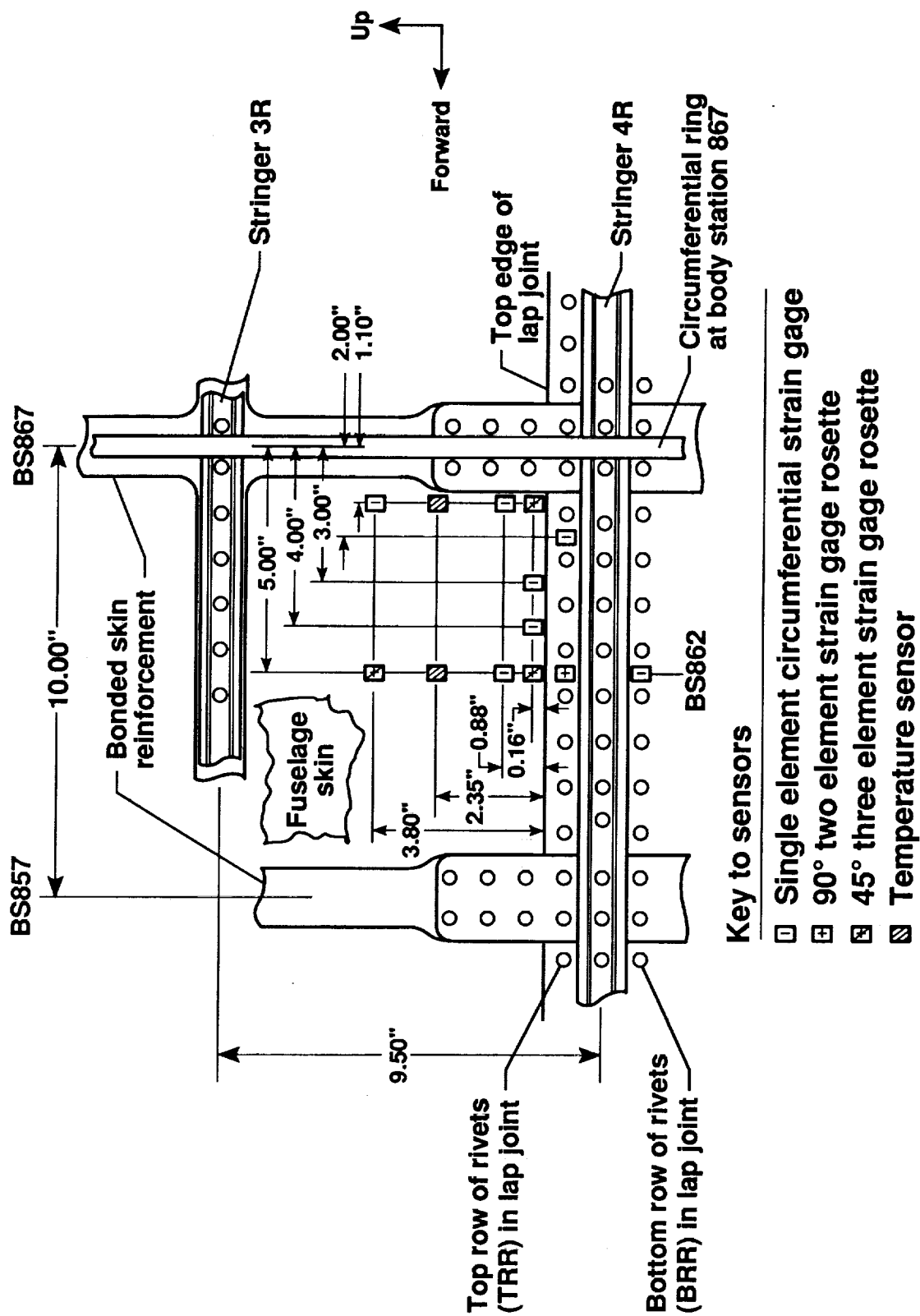


Figure 2. Locations of strain gages and temperature sensors relative to structural members on the inside of fuselage.

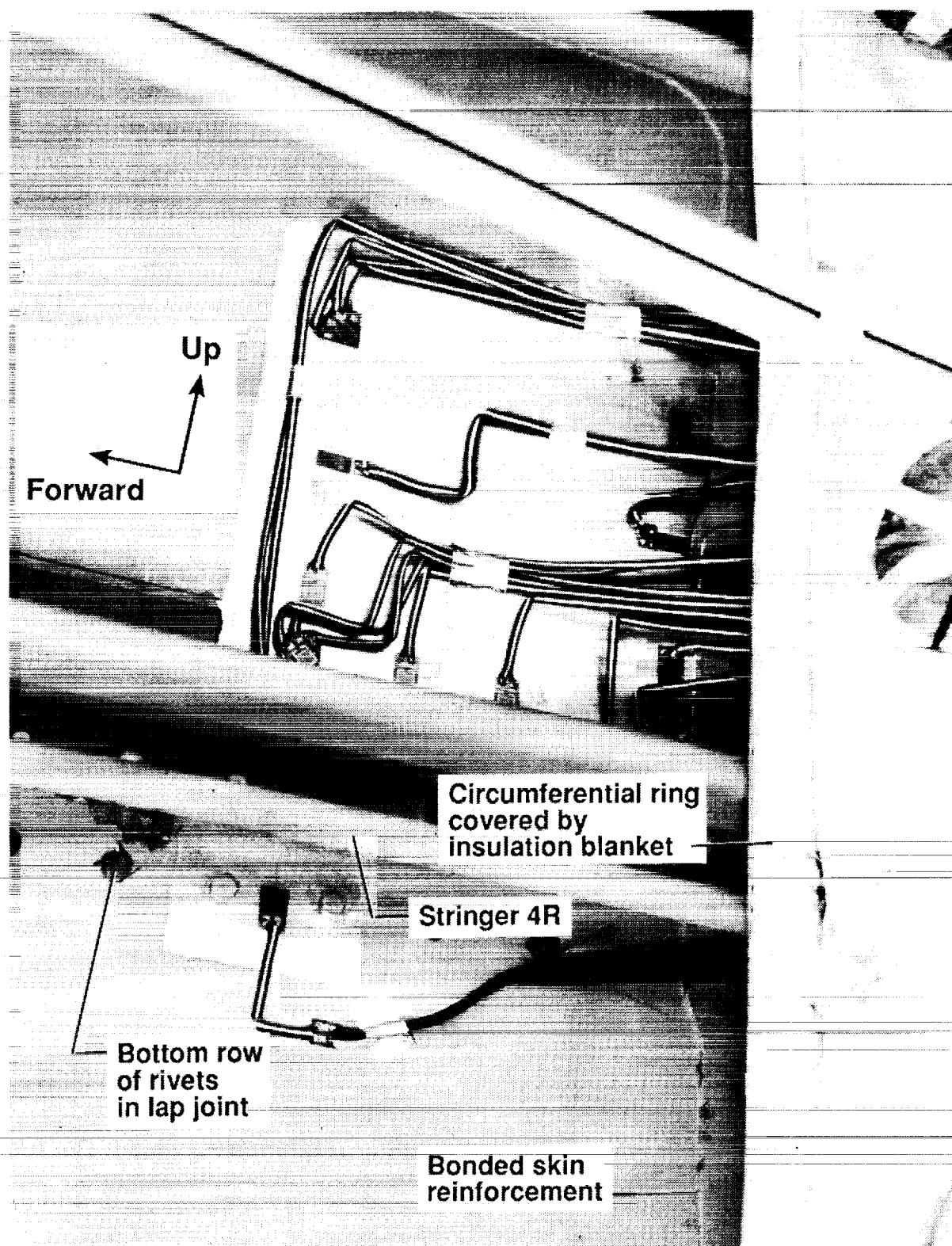
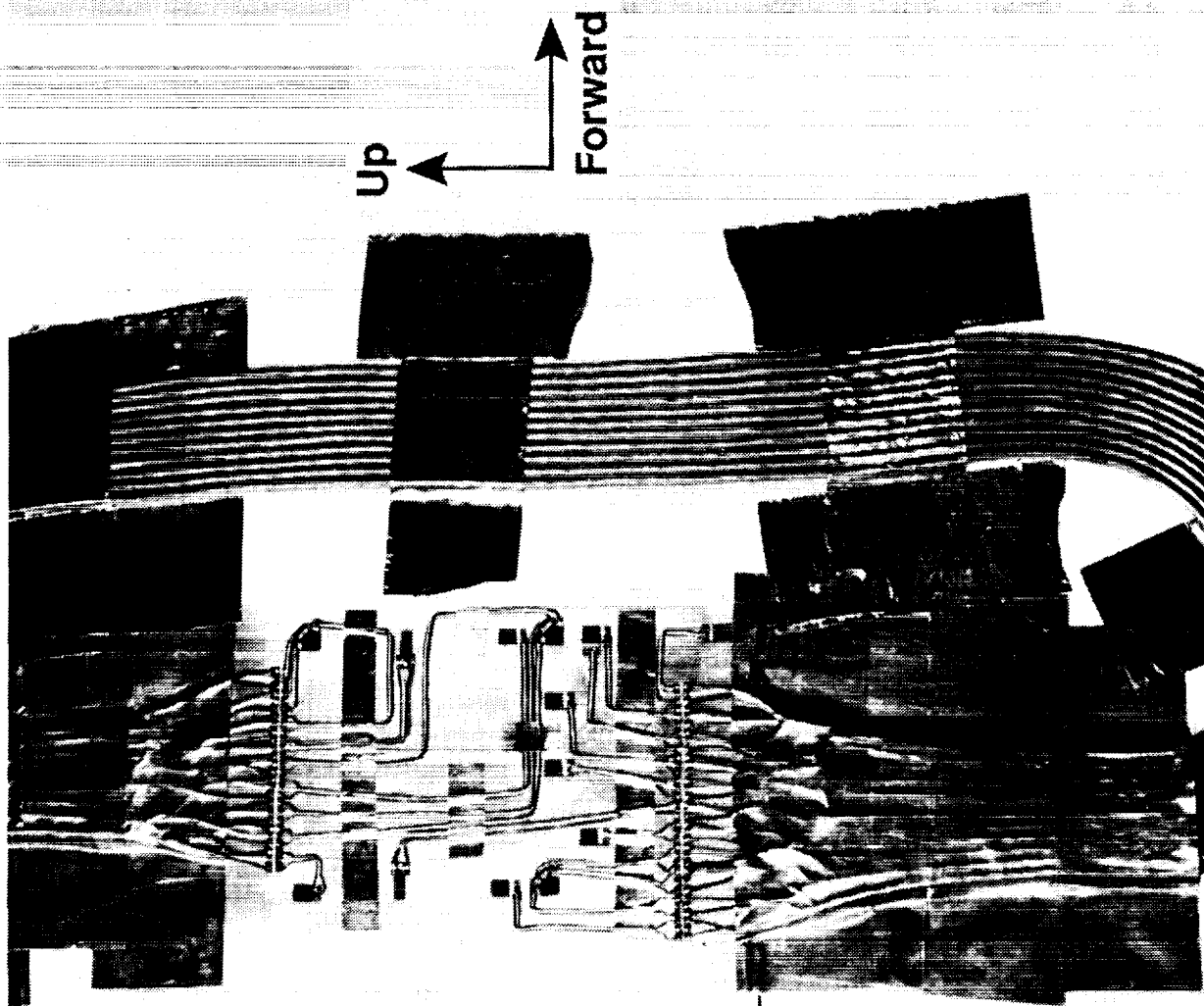


Figure 3(a). Photograph of strain gage and temperature sensor installations on the inside of fuselage



Bottom edge
of lap joint

Figure 3(b). Photograph of strain gage and temperature sensor installations on the outside of fuselage

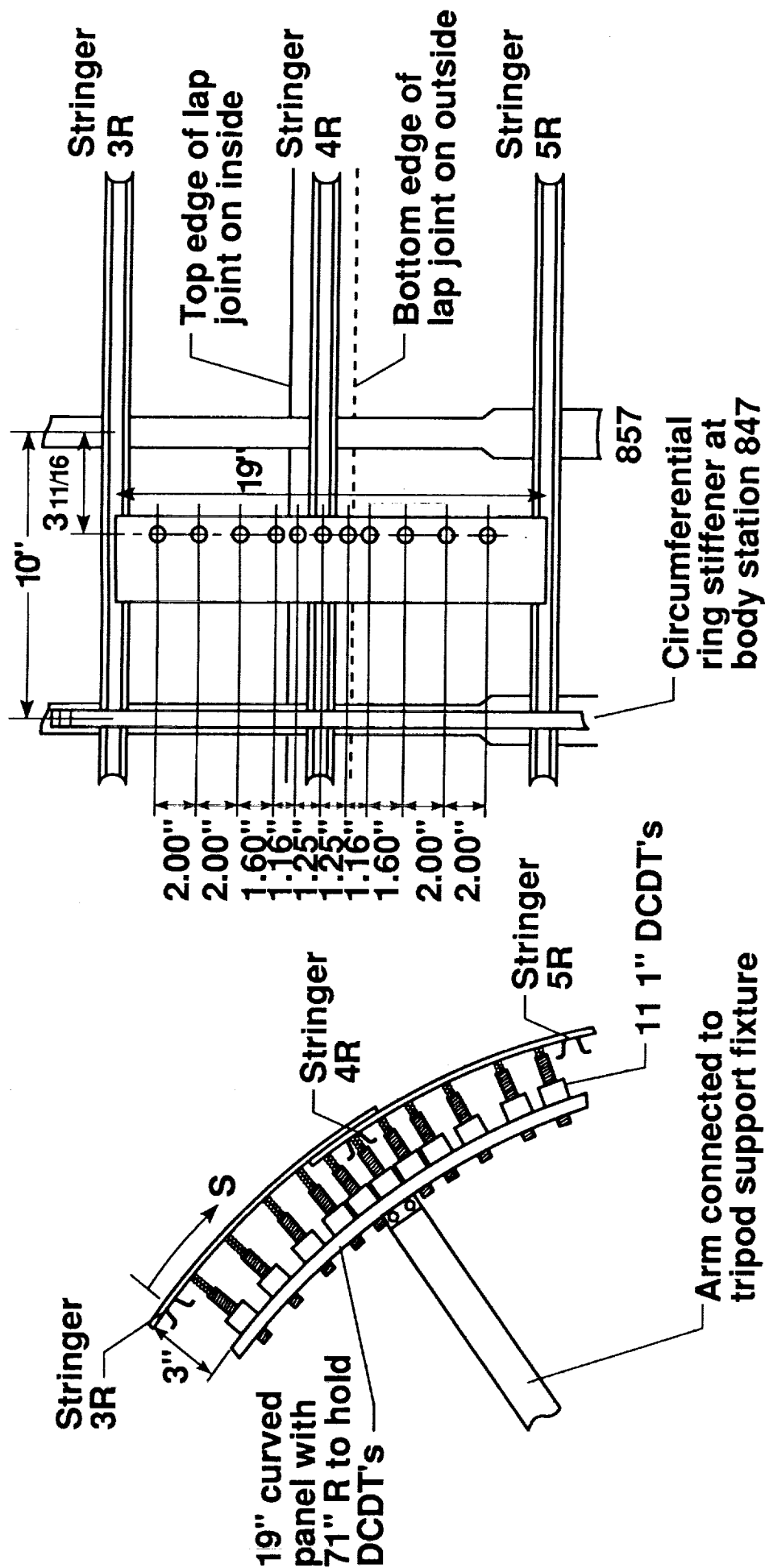


Figure 4. Location of direct current differential transformers relative to structural members on the inside of the fuselage.

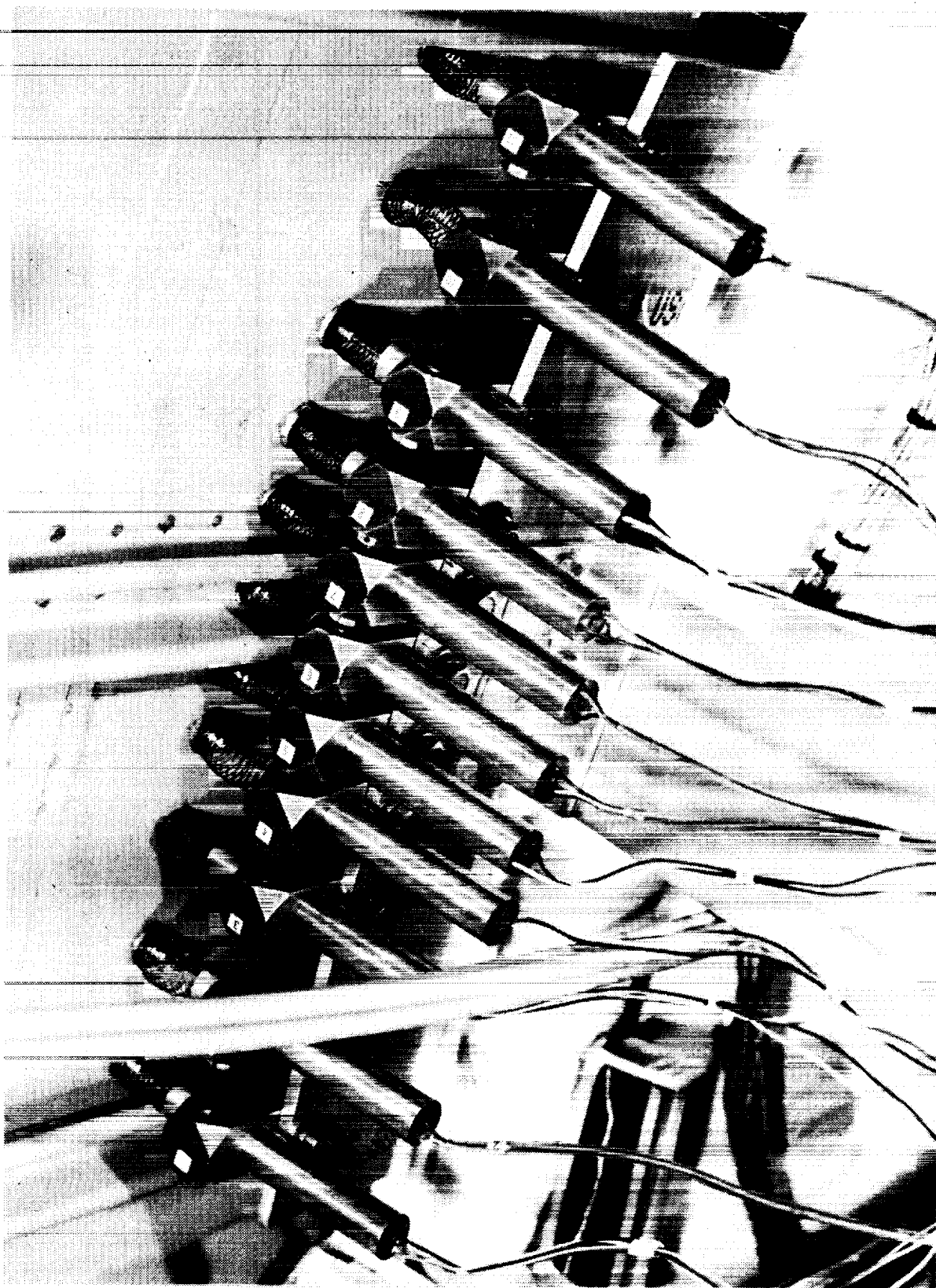


Figure 5. Photograph of DCDT arrangement on interior of fuselage.

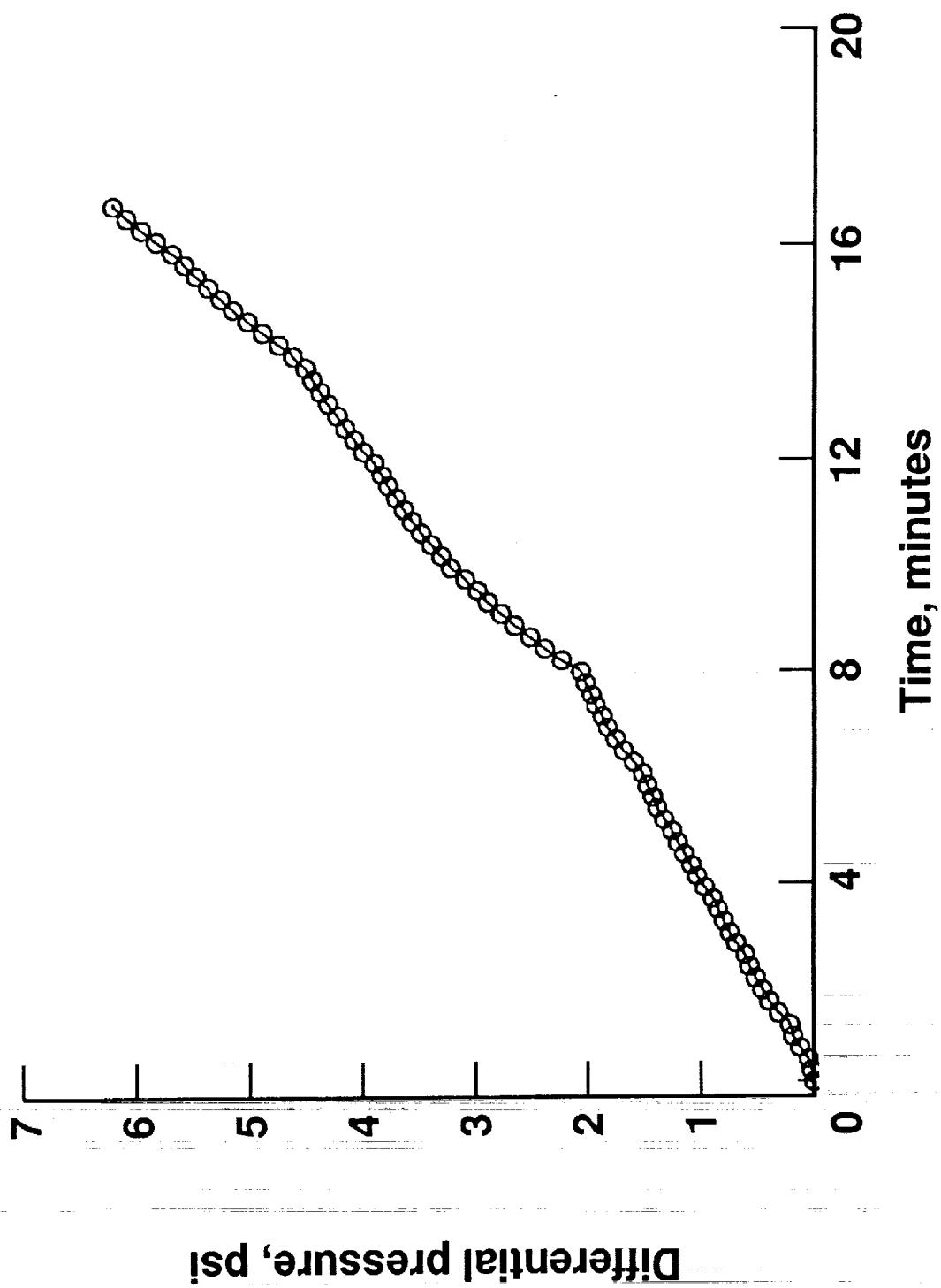


Figure 6. Time history of differential pressure during test.

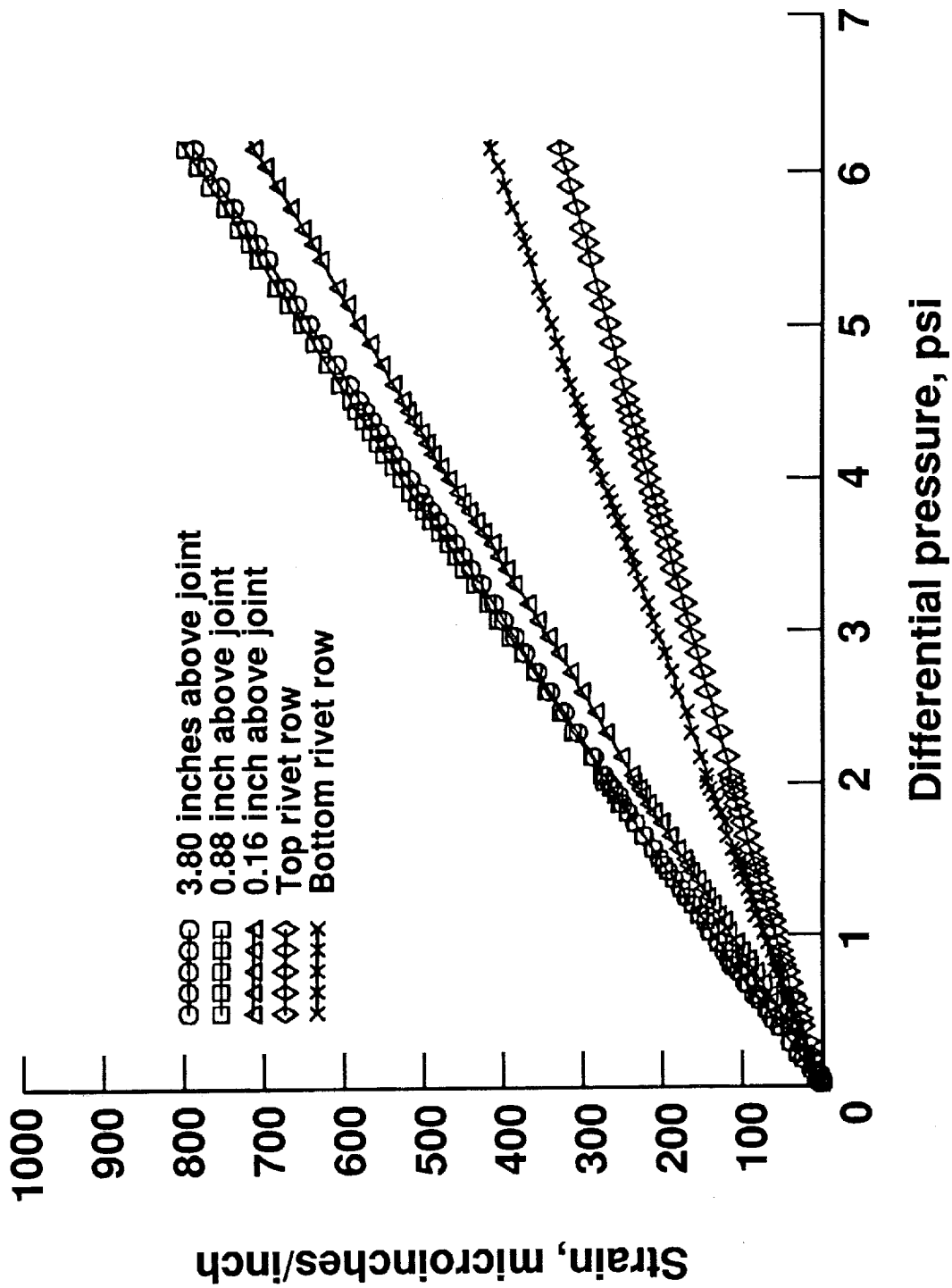


Figure 7(a). Membrane strains in the hoop direction at BS862 as a function of differential pressure.

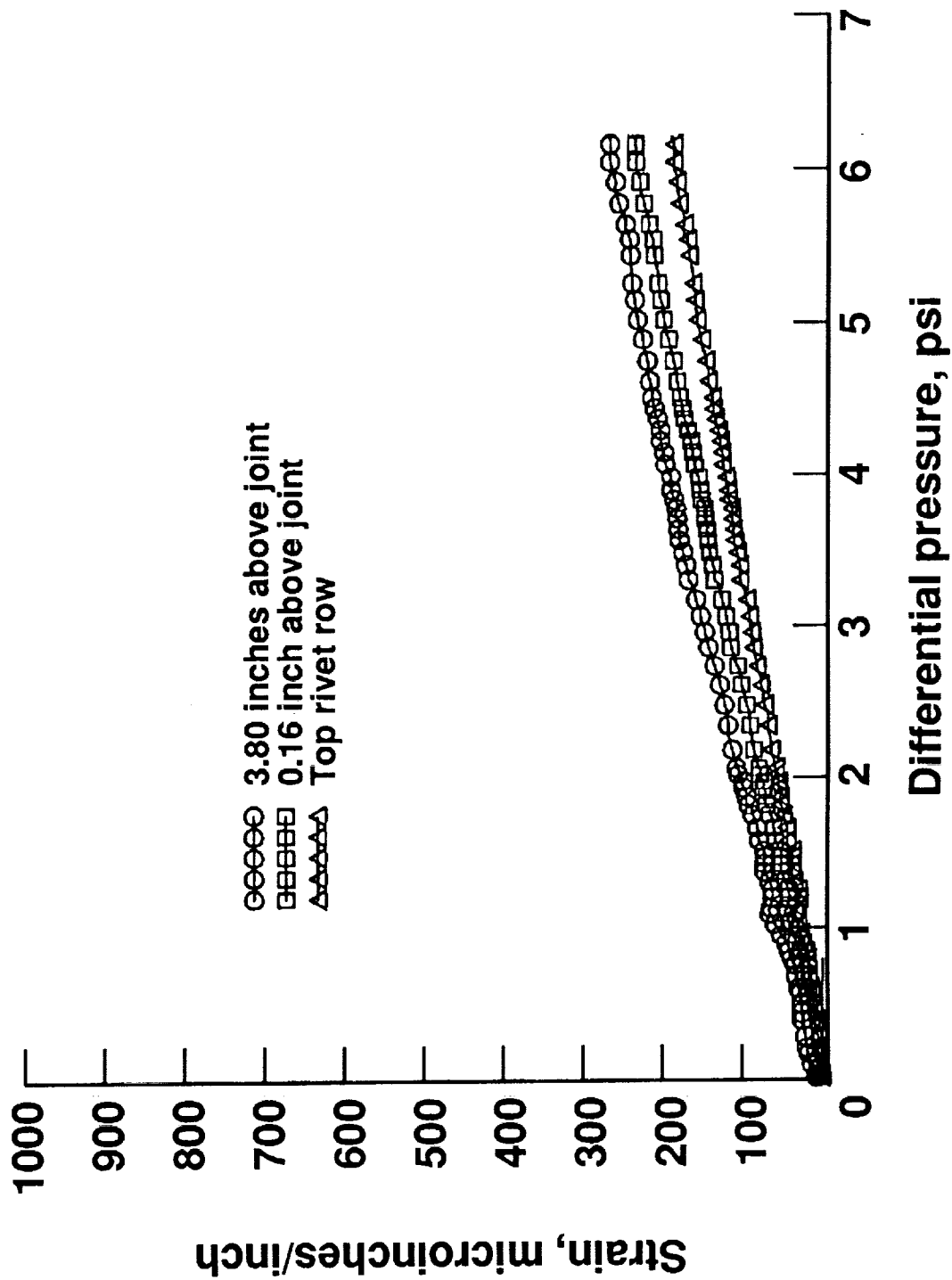


Figure 7(b). Membrane strains in the longitudinal direction at BS862 as a function of differential pressure.

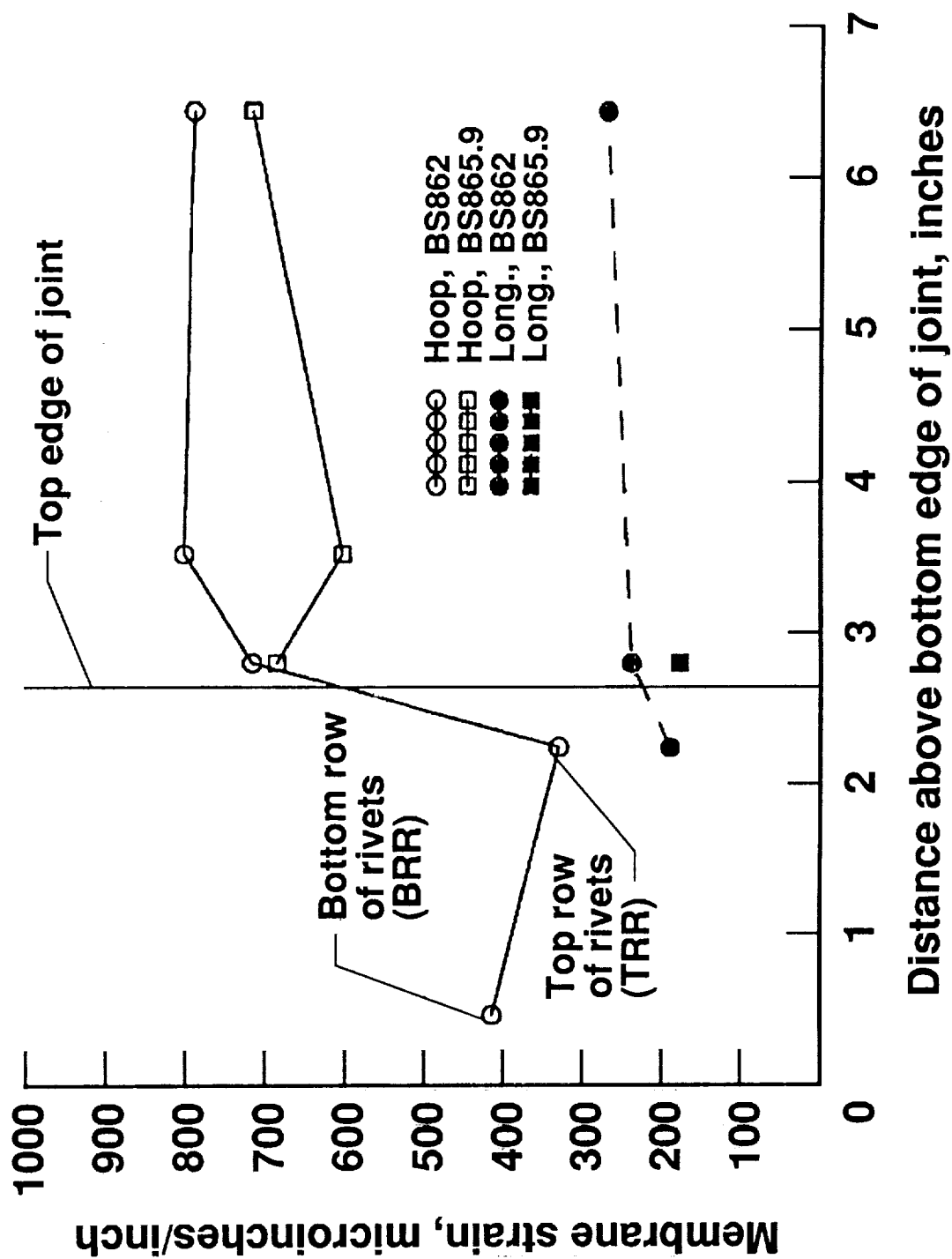


Figure 8. Membrane strains in the hoop and longitudinal directions at BS862 and BS865.9 at a differential pressure of 6.2 psi as a function of vertical location relative to the joint.

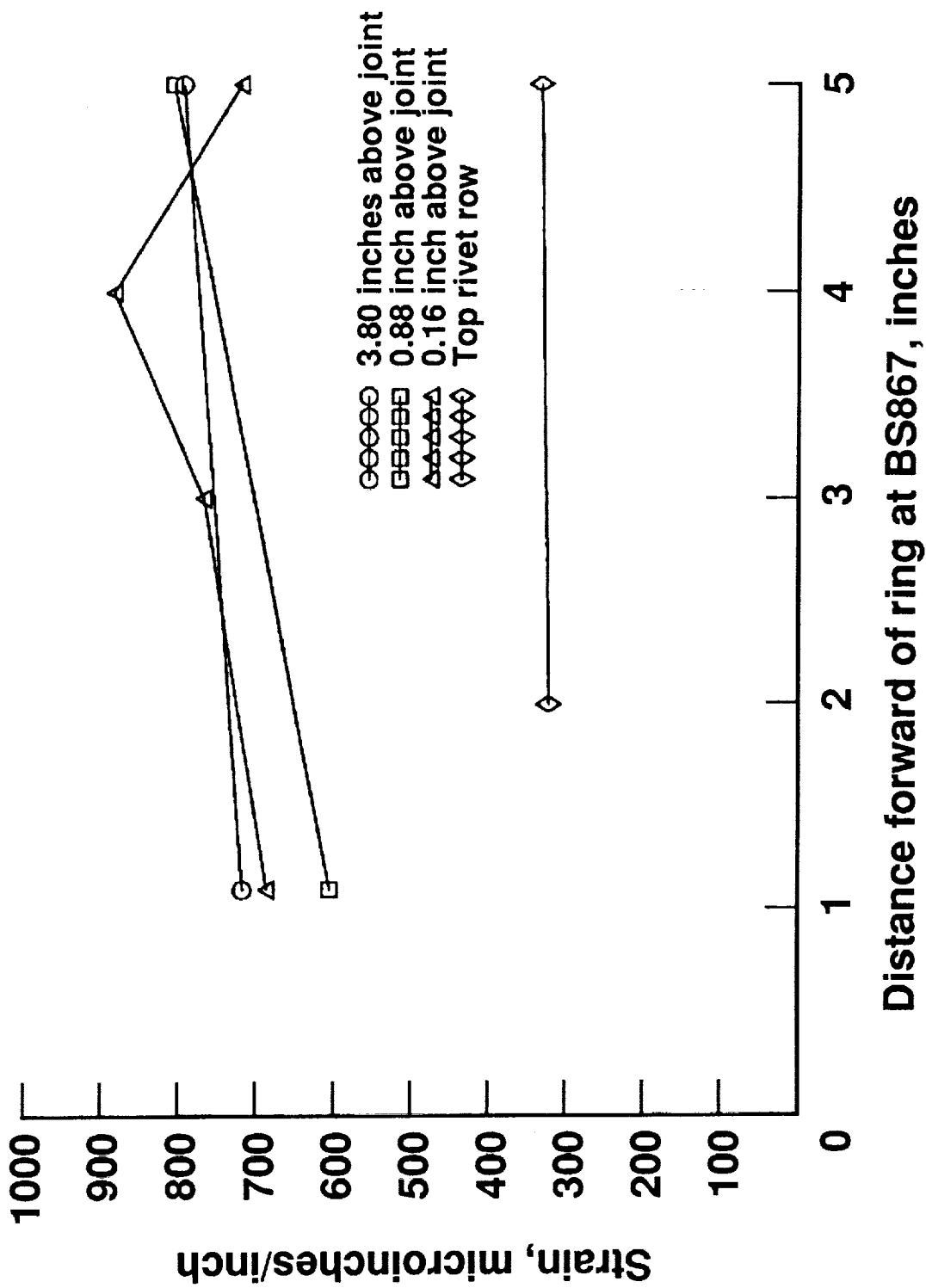


Figure 9. Membrane strains in the hoop direction at a differential pressure of 6.2 psi as a function of distance from the ring stiffener at BS867.

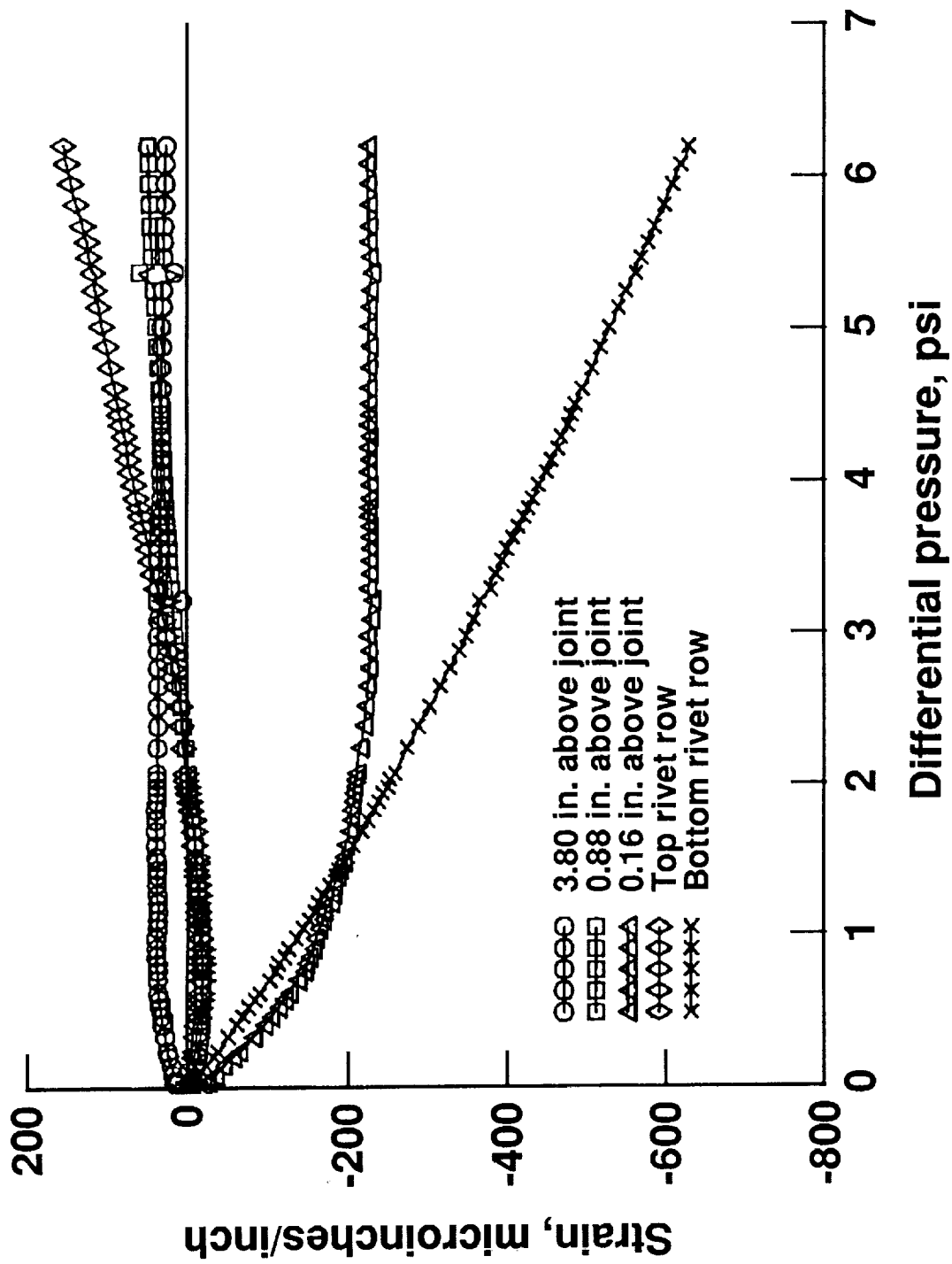


Figure 10(a). Bending strains in the hoop direction at BS862 as a function of differential pressure.

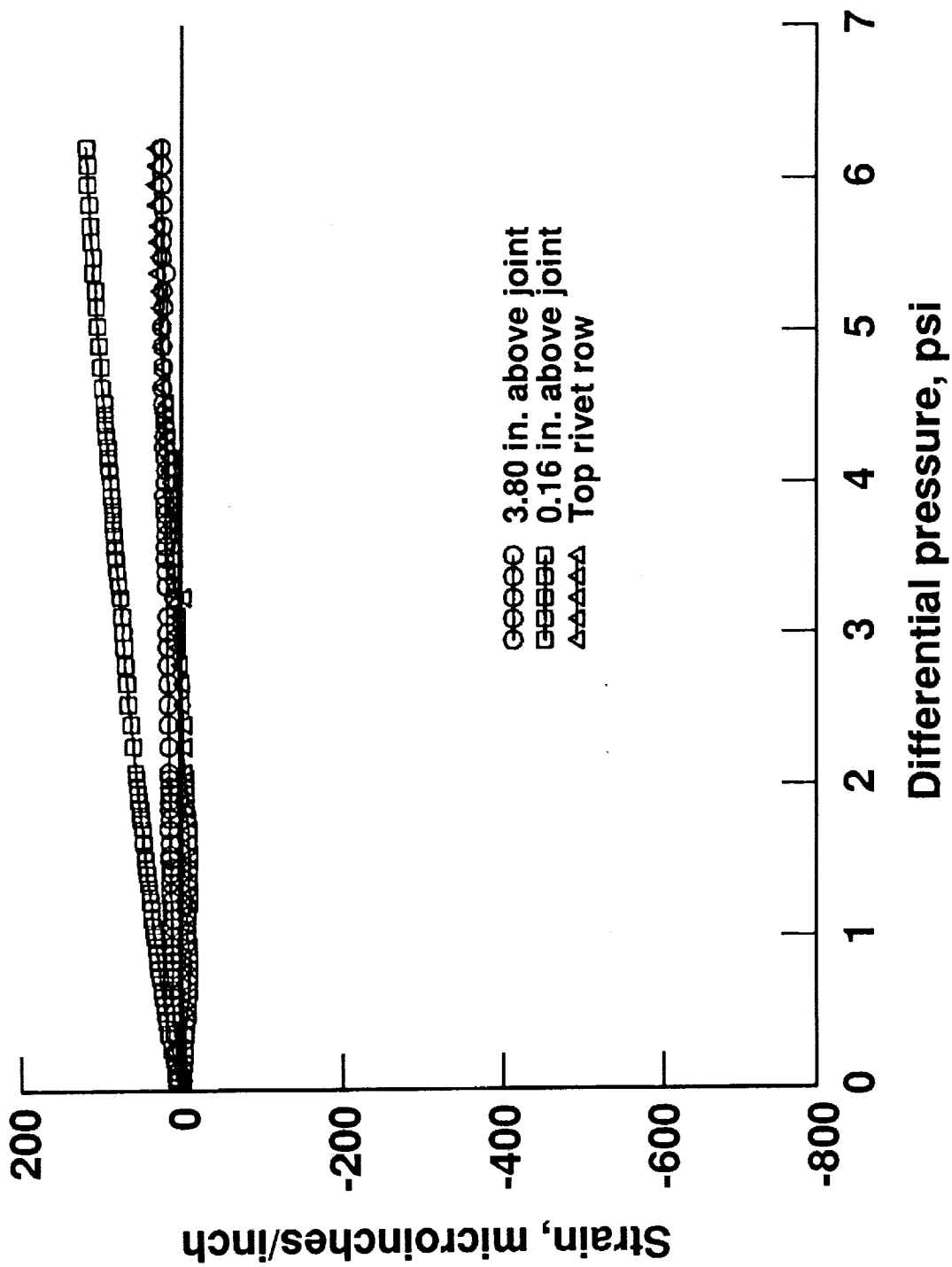


Figure 10(b). Bending strains in the longitudinal direction at BS862 as a function of differential pressure.

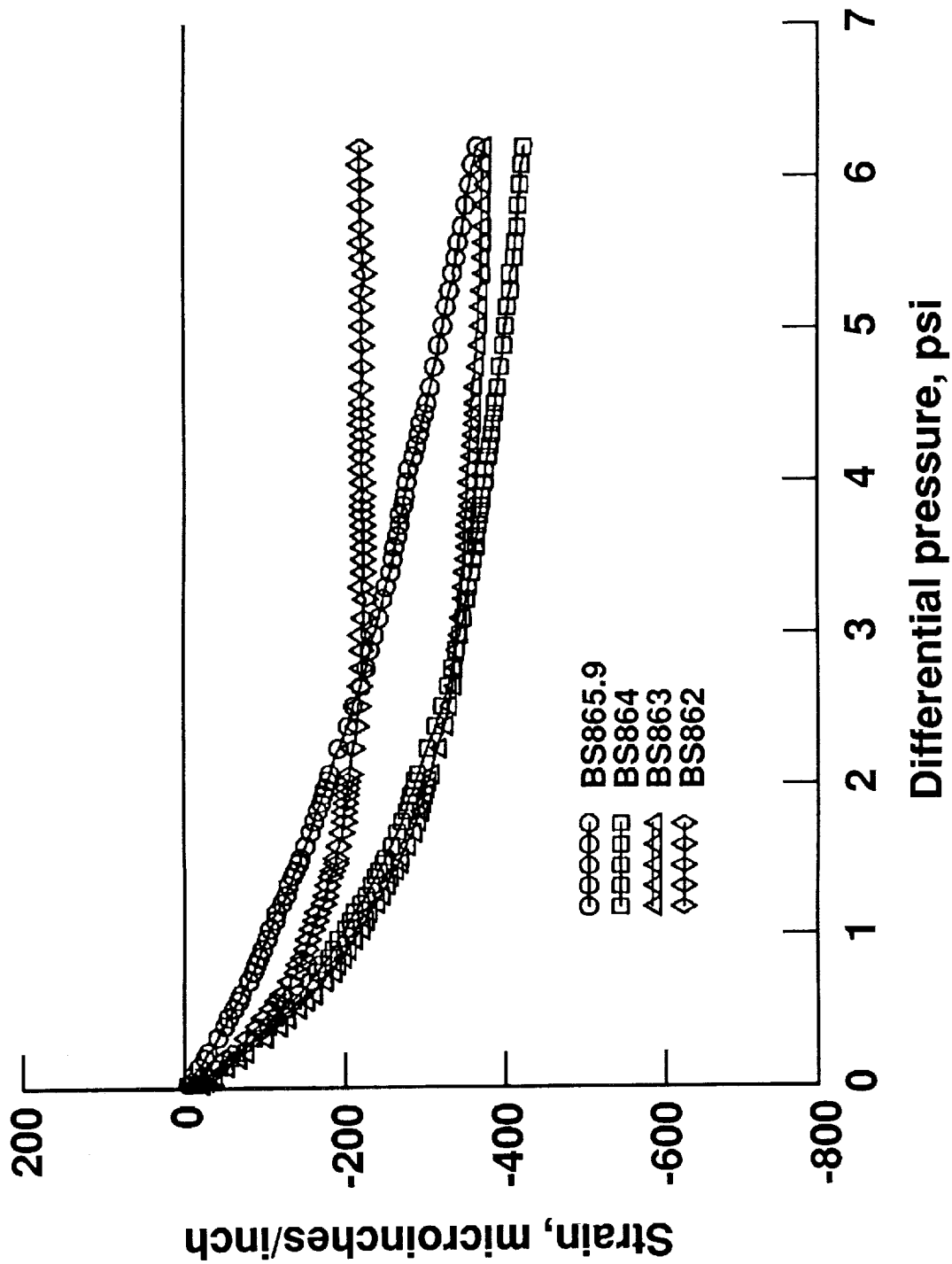


Figure 11. Bending strains in the hoop direction at 0.16 inch above the joint at several body stations as a function of differential pressure.

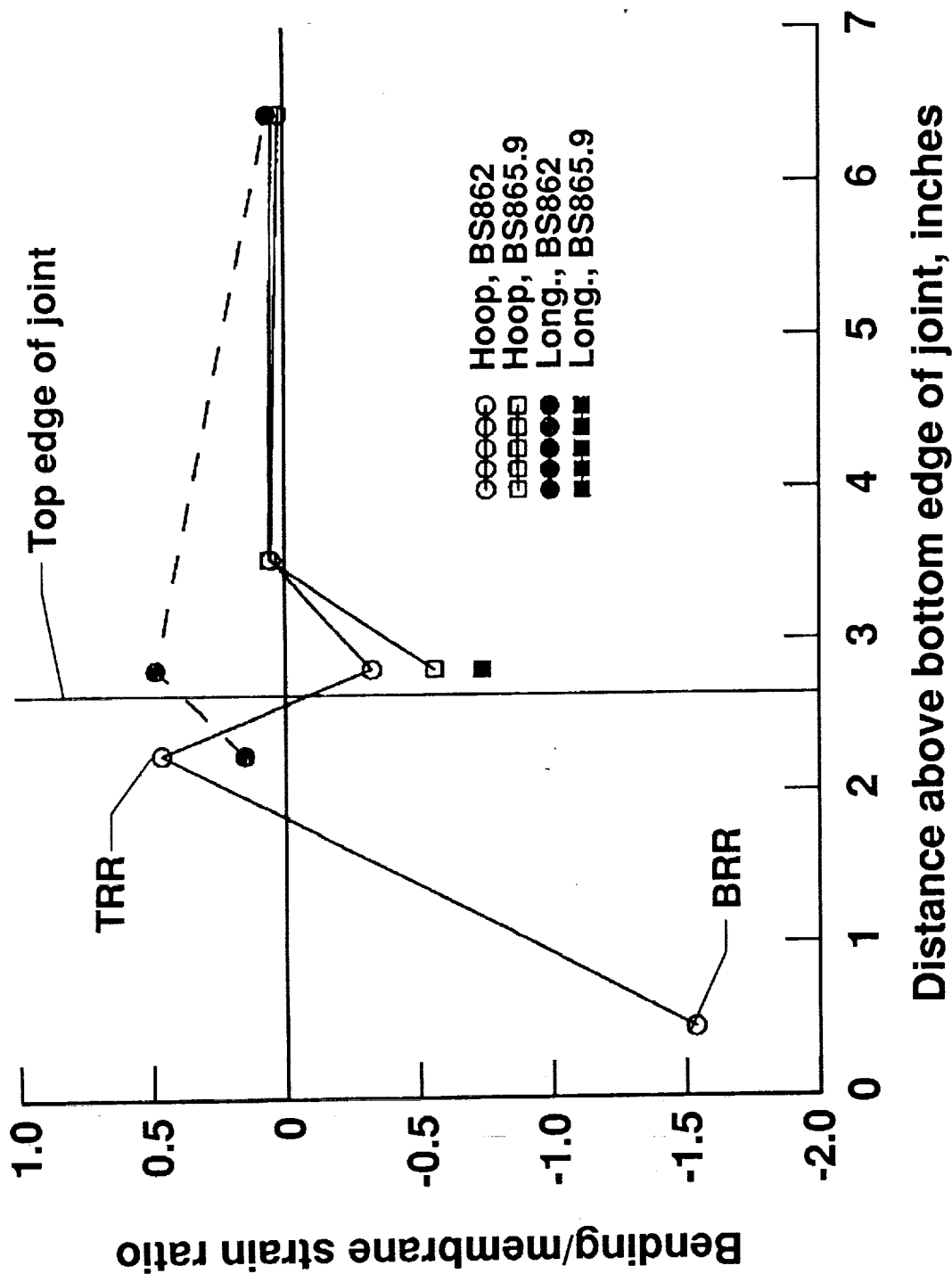


Figure 12. Ratios of bending to membrane strains in the hoop and longitudinal directions at BS862 and BS865.9 at a differential pressure of 6.2 psi as a function of vertical location relative to the joint.

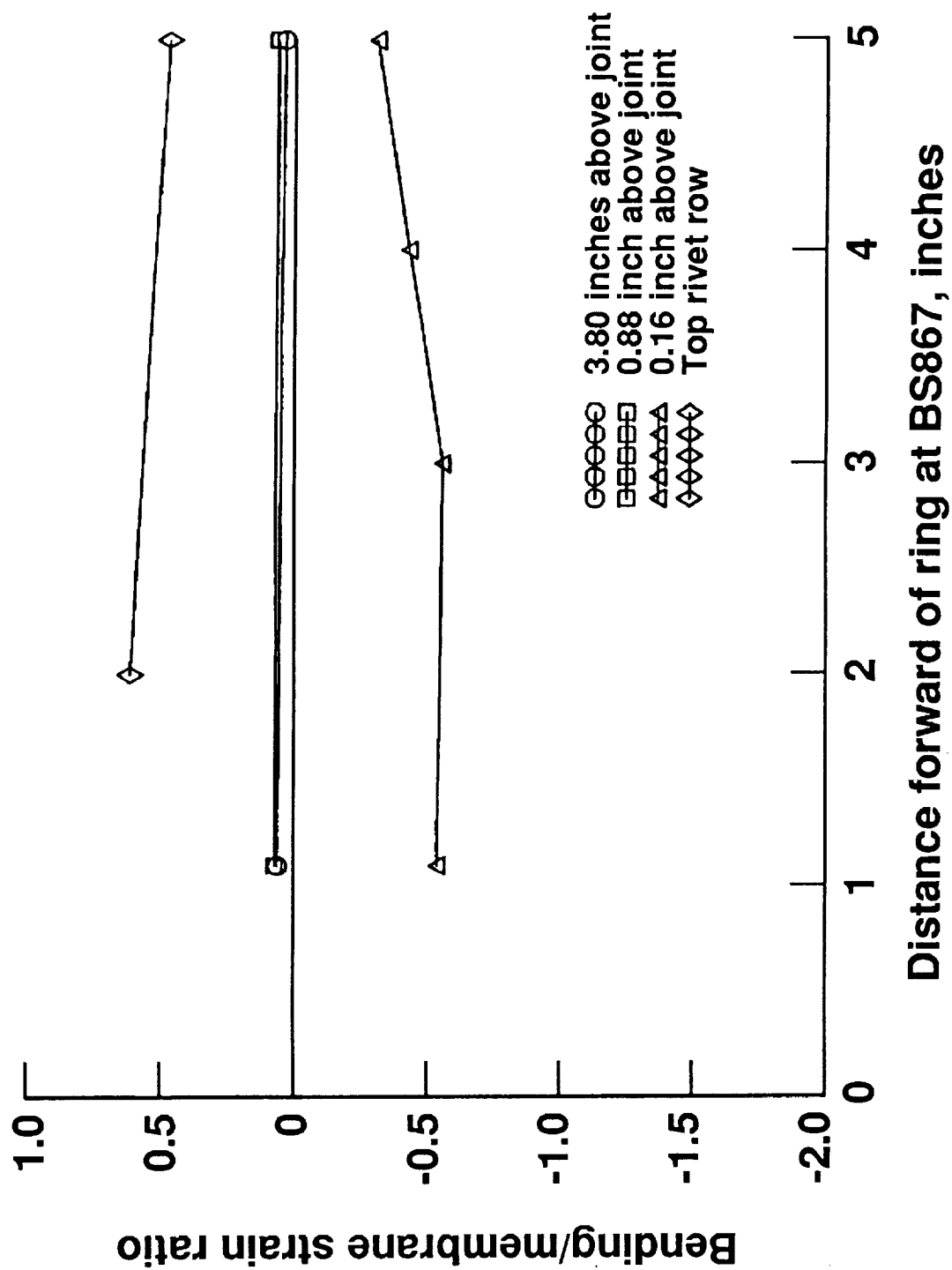


Figure 13. Ratios of bending to membrane strains in the hoop direction at a differential pressure of 6.2 psi as a function of distance from the ring stiffener at BS867.

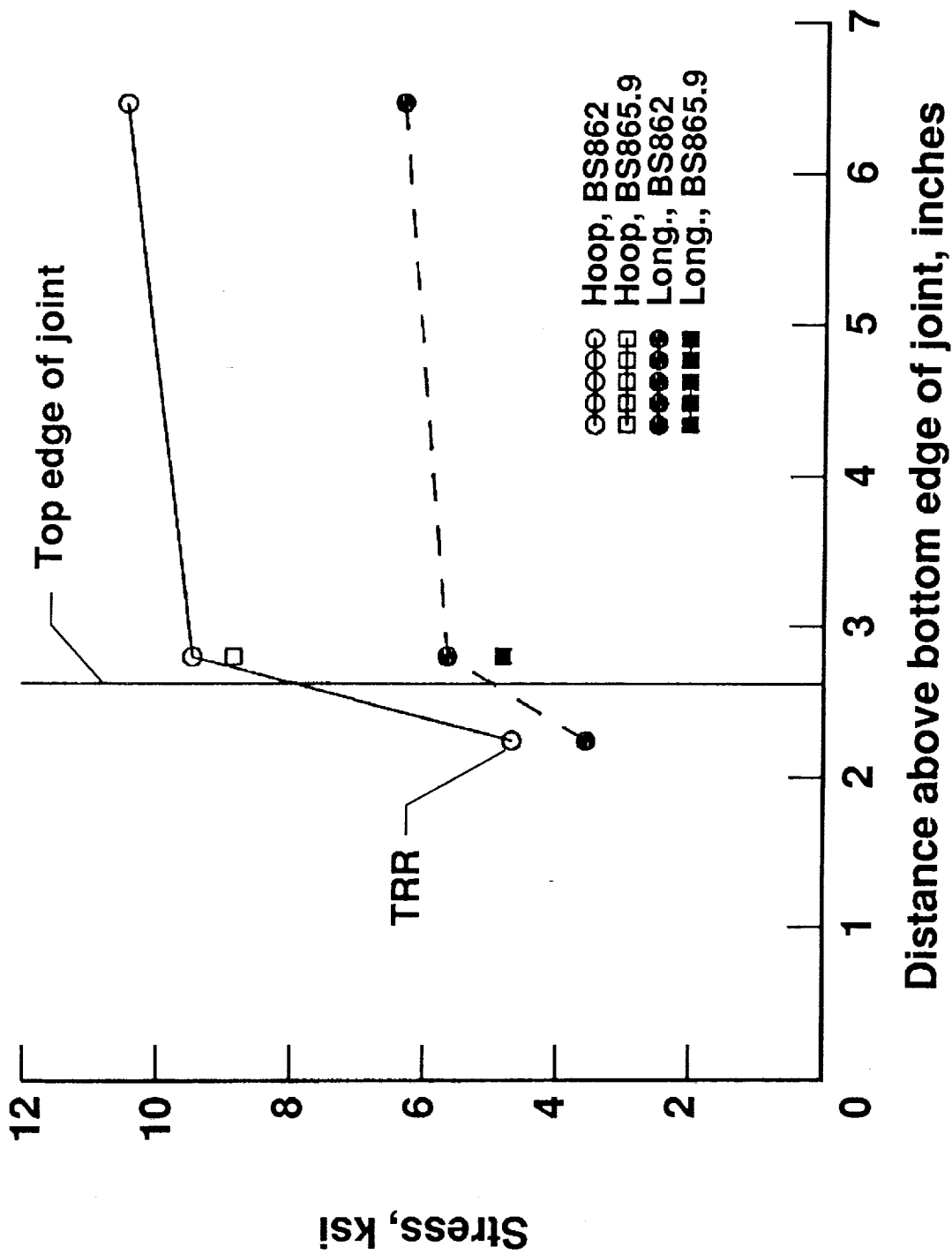


Figure 14. Membrane stresses in the hoop and longitudinal directions at BS862 and BS865.9 at a differential pressure of 6.2 psi as a function of vertical location relative to the joint.

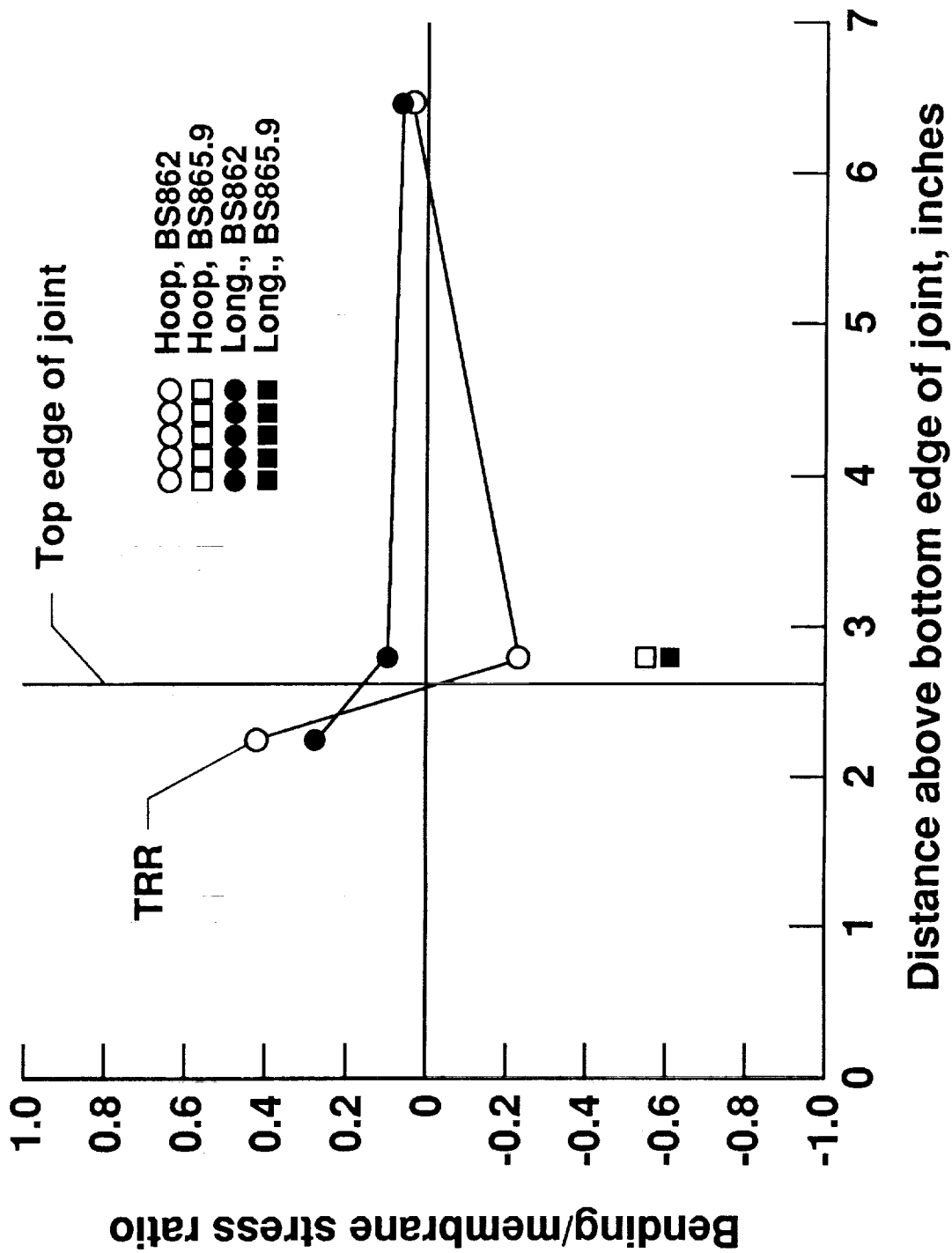


Figure 15. Ratios of bending to membrane stresses in the hoop and longitudinal directions at BS862 and BS865.9 at a differential pressure of 6.2 psi as a function of vertical location relative to the joint.

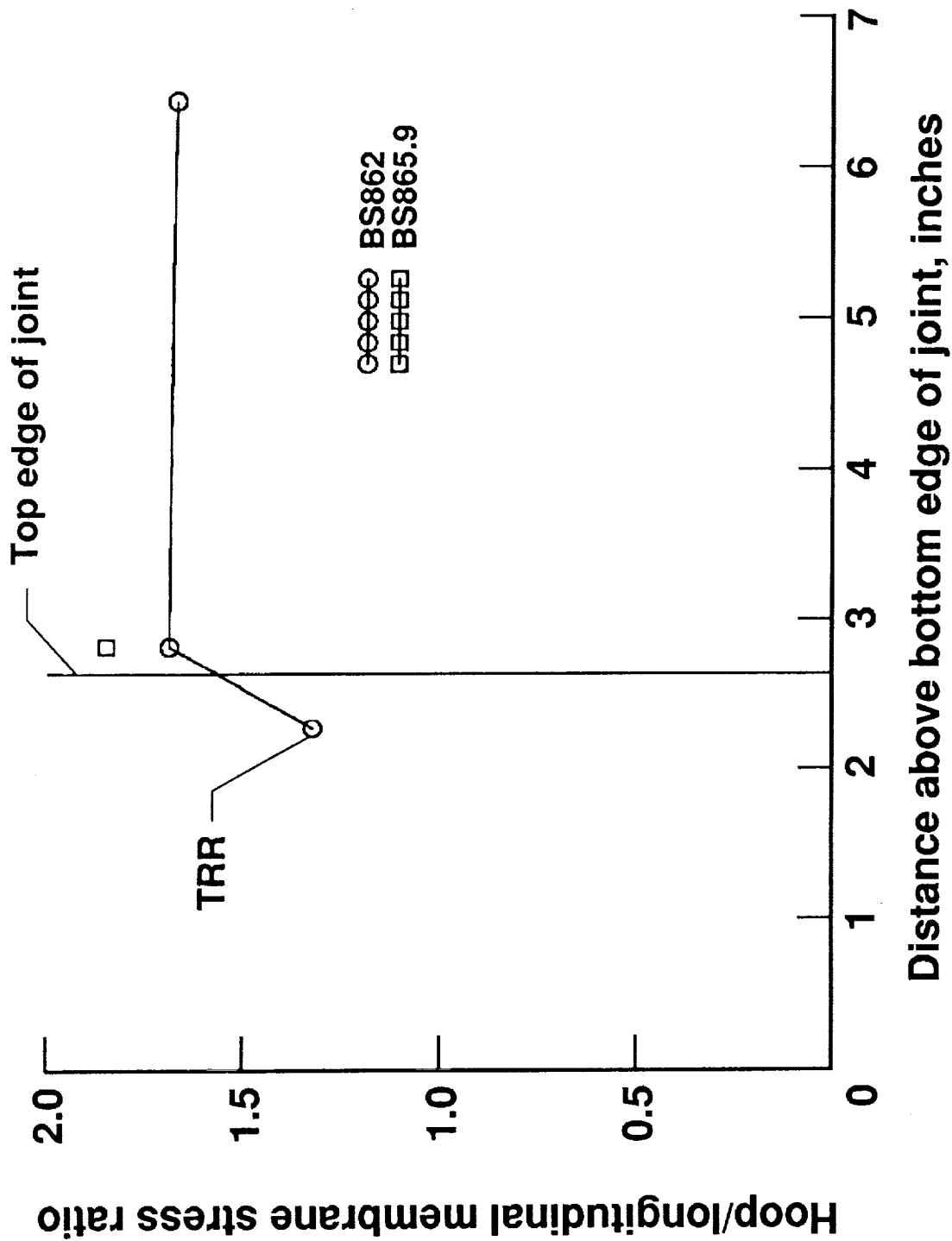


Figure 16. Ratio of hoop to longitudinal membrane stresses at BS862 and BS865.9 at a differential pressure of 6.2 psi as a function of vertical location relative to the joint.

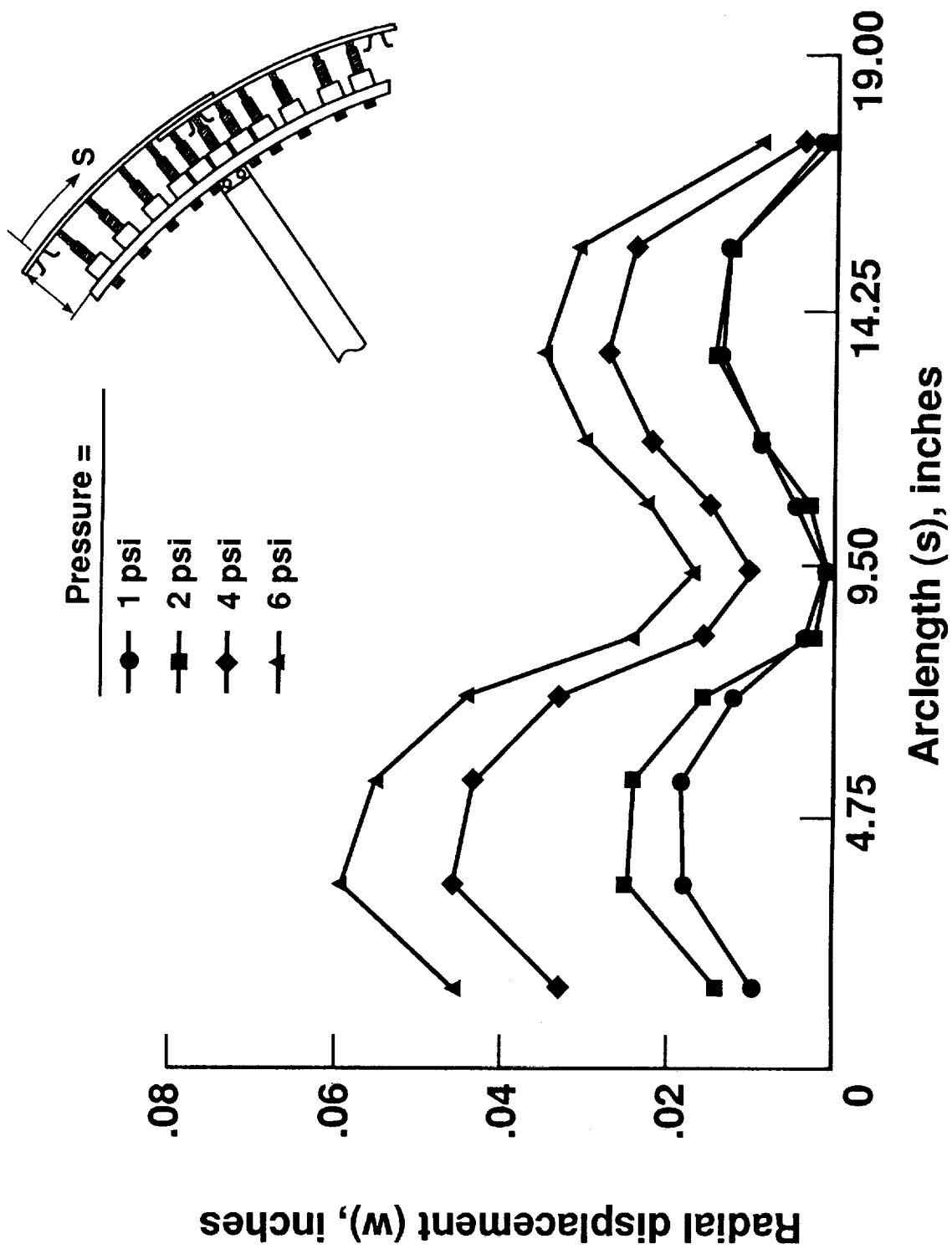


Figure 17. Radial displacement of fuselage skin across lap joint.

REPORT DOCUMENTATION PAGEForm Approved
OMB No. 0704-0188

Public reporting burden for this collection of information is estimated to average 1 hour per response, including the time for reviewing instructions, searching existing data sources, gathering and maintaining the data needed, and completing and reviewing the collection of information. Send comments regarding this burden estimate or any other aspect of this collection of information, including suggestions for reducing this burden, to Washington Headquarters Services, Directorate for Information Operations and Reports, 1215 Jefferson Davis Highway, Suite 1204, Arlington, VA 22202-4302, and to the Office of Management and Budget, Paperwork Reduction Project (0704-0188), Washington, DC 20503.

1. AGENCY USE ONLY (Leave blank)		2. REPORT DATE October 1991	3. REPORT TYPE AND DATES COVERED Technical Memorandum	
4. TITLE AND SUBTITLE Measurements of Fuselage Skin Strains and Displacements Near a Longitudinal Lap Joint in a Pressurized Aircraft			5. FUNDING NUMBERS 505-63-10-03	
6. AUTHOR(S) Edward P. Phillips and Vicki O. Britt				
7. PERFORMING ORGANIZATION NAME(S) AND ADDRESS(ES) NASA Langley Research Center Hampton, VA 23665-5225			8. PERFORMING ORGANIZATION REPORT NUMBER	
9. SPONSORING/MONITORING AGENCY NAME(S) AND ADDRESS(ES) National Aeronautics and Space Administration Washington, DC 20546			10. SPONSORING/MONITORING AGENCY REPORT NUMBER NASA TM-104163	
11. SUPPLEMENTARY NOTES				
12a. DISTRIBUTION/AVAILABILITY STATEMENT Unclassified - Unlimited Subject Category - 39			12b. DISTRIBUTION CODE	
13. ABSTRACT (Maximum 200 words) Strains and displacements in a small area near a longitudinal lap joint in the fuselage skin of a B737 aircraft were measured during a pressurization cycle to a differential pressure of 6.2 psi while the aircraft was on the ground. Strain gages were placed on both the inside and outside surfaces of the fuselage at the same locations. Direct Current Differential Transformers (DCDTS) were distributed circumferentially across the lap joint on the inside of the aircraft to measure the relative radial displacements of the skin. The major trends in the results were: (1) hoop strains were higher than longitudinal strains at each location, (2) membrane strains in the unreinforced skin were higher than in the joint, (3) membrane strains in the hoop direction, as well as radial displacements, tended to be highest at the mid-bay location between skin reinforcements, (4) significant bending in the hoop direction occurred in the joint and in the skin near the joint, and the bending was unsymmetrically distributed about the stringer at the middle of the joint, and (5) the radial displacements were unsymmetrically distributed across the lap joint. The interpretation of the strain gage data for locations on the bonded and riveted lap joint assumed that the joint did not contain disbanded areas.				
14. SUBJECT TERMS Aircraft structures; Ground tests; Fuselages; Lap joints; Structural strain; Bending; Deflection			15. NUMBER OF PAGES 28	
			16. PRICE CODE AO3	
17. SECURITY CLASSIFICATION OF REPORT Unclassified	18. SECURITY CLASSIFICATION OF THIS PAGE Unclassified	19. SECURITY CLASSIFICATION OF ABSTRACT	20. LIMITATION OF ABSTRACT	